

## SPARSITY-BASED RADAR IMAGING OF BUILDING STRUCTURES

*Eva Lagunas<sup>1</sup>, Moeness G. Amin<sup>2</sup>, Fauzia Ahmad<sup>2</sup> and Montse Najar<sup>1</sup>*

<sup>1</sup> Universitat Politècnica de Catalunya (UPC), Barcelona, Spain

<sup>2</sup> Radar Imaging Lab, Center for Advanced Communications  
Villanova University, Villanova, PA 19085, USA

### ABSTRACT

**In this paper, we address imaging of the interior structure of a building using a reduced number of measurements in through-the-wall imaging and urban sensing applications. Unlike majority of the feature detection methods that are applied in the image domain, the proposed approach works in the data domain and exploits prior information of construction practices together with the sparsity described by the features. More specifically, the interior walls are assumed to be either parallel or perpendicular to the front wall and a dictionary of possible wall locations is proposed as a sparse representation of the scene. Compressive sensing is then applied to the reduced set of observations to recover the true positions of the walls. Supporting results based on laboratory experiments are provided.**

### 1. INTRODUCTION

Through-the-wall Radar Imaging (TWRI) is an emerging technology that allows inspection of building interiors from outside through the walls [1]. TWRI combines electromagnetic waves transmitted and received at several different locations along an array aperture, either real or synthetic, to obtain two-dimensional images of the region of interest located behind the front wall. High resolution imaging is achieved if large bandwidth signals and long antenna arrays are used. However, this implies acquisition and processing of large amounts of data volume. To alleviate the data acquisition and processing bottlenecks, Compressive Sensing (CS) has emerged as an effective approach that allows compression of the data while it is sampled [2, 3]. Decreasing the number of acquired samples can also be helpful in TWRI from a logistic point of view, as some of the data measurements in space and frequency can be difficult, or impossible to attain.

In this paper, we address the problem of imaging building interior structures using a reduced number of measurements. Backprojection is the conventional method used in TWRI for

image formation. Although it provides good quality scene reconstructions when the full data volume is available, back-projection has been shown to compromise the image quality when a reduced number of data samples is considered [4], thereby impeding the detection of targets behind the wall in the image domain. Further, the presence of interior structures in the scene together with indoor objects generates multipath reflections, which perturb the sensed backscatter making the problem even more challenging. Here, we propose a sparsifying basis for the determination of the building layout, which is based on prior knowledge about common construction practices. The building layout is usually composed of exterior and interior walls which are parallel or perpendicular to each other. Therefore, building layout estimation can be posed as a feature detection problem where the features are the walls. Feature detection of through-the-wall objects is usually developed in the image-domain because it has been shown to handle multiple targets without prior assumptions on target radar cross section (RCS) [5]. Omitting the image formation step is the most attractive advantage of the data-domain based detection approach, which, however, involves transmit waveform design incorporating some prior knowledge of the target RCS [6]. This paper presents a new method to detect multiple walls in the data-domain using a small number of observations without making any assumptions regarding the target RCS. The proposed approach takes advantage of prior information about common construction practices together with the sparsity described by the features. More specifically, given the assumption that the interior walls are parallel or perpendicular to the front wall, a dictionary of possible wall locations is proposed as a sparse representation of the scene. CS is then applied to the reduced set of observations to recover the positions of the various walls. The proposed method can be considered as a sparsity-based modification of the well-known Radon Transform (RT) [7], where, instead of projecting onto all possible slanted lines, we project only onto a particular line direction. Similar approaches were recently proposed in [8, 9]. In [8], the Hough Transform (HT) domain for continuous infinite-length line detection was strictly discretized for tunnel detection in Ground Penetrating Radar (GPR). Neither any knowledge of the direction of lines was considered nor the extent of the lines was determined. Al-

This work was supported by ONR under grants N00014-11-1-0576 and N0014-10-1-0455.

E. Lagunas is partially supported by the fellowship FI-DGR-2012.

though the TWRI problem is considered in [9], it does not deal with a reduced data volume and provides an improvement to the conventional HT reconstruction using the full set of measurements under assumption of the knowledge of the direction of walls by applying sharp windowing to the resulting HT.

The remainder of the paper is organized as follows. Section 2 describes the point-target based signal model for through-the-wall radar imaging. In Section 3, a sparsifying dictionary, which exploits prior information about common construction practices, is designed to cater to imaging of extended targets. Section 4 provides the fundamental equations for imaging of walls from a few data observations. Results for simulated and experimental data are discussed in Section 5. Section 6 states the conclusions.

## 2. TWRI SIGNAL MODEL

Consider an  $N$ -element line array located parallel to the front wall along the  $x$ -axis, as shown in Fig. 1. Let the  $n$ th transceiver illuminate the scene with a stepped-frequency signal of  $M$  frequencies. The reflections by the wall and any targets in the scene are measured only at the same transceiver location. Let  $\omega_0$  and  $\Delta_\omega$  denote the lowest frequency in the bandwidth spanned by the stepped-frequency signal, and the frequency step size, respectively. For a scene consisting of  $P$  point targets, the signal received by the  $n$ th transceiver corresponding to the  $m$ -th frequency,  $\omega_m = \omega_0 + m\Delta_\omega$  with  $m = 0, \dots, M - 1$ , can be expressed as,

$$y(m, n) = \sigma_w e^{-j\omega_m \tau_w} + \sum_{p=0}^{P-1} \sigma_p e^{-j\omega_m \tau_{p,n}} \quad (1)$$

where  $\sigma_w$  and  $\sigma_p$  are the complex reflectivity of the wall and the  $p$ th target, respectively, and  $\tau_w$  and  $\tau_{p,n}$  are the two-way traveling time of the signal from the  $n$ th antenna to the wall and between the  $n$ th antenna and the  $p$ th target, respectively. As the wall is a specular reflector and the sensors are located parallel to the front wall, the delay  $\sigma_w$  does not depend on the variable  $n$ .

Assume that the scene being imaged is divided into a finite number of grid-points in crossrange and downrange. That is, the scene can be represented by the reflectivity function  $r(k, l)$ ,  $k = 0, \dots, N_x - 1$ ,  $l = 0, \dots, N_z - 1$ . Let  $\mathbf{y}_n$  represent the received signal vector corresponding to the  $M$  frequencies and the  $n$ th transceiver location, and  $\mathbf{r}$  be the concatenated  $N_x N_z \times 1$  scene reflectivity vector corresponding to the spatial sampling grid. Then, assuming a scene composed of point targets and using eqn. (1), we obtain the matrix-vector form

$$\mathbf{y}_n = \Psi_n \mathbf{r} \quad (2)$$

where  $\Psi_n$  is an  $M \times N_x N_z$  matrix, whose rows are given by,

$$[\Psi_n]_m = [e^{-j\omega_m \tau_{n,(0,0)}} \quad \dots \quad e^{-j\omega_m \tau_{n,(N_x-1, N_z-1)}}] \quad (3)$$

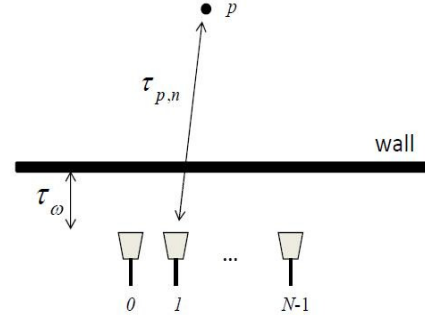


**Fig. 1.** Data collection using a virtual array in through-the-wall radar imaging.

and  $\tau_{n,(k,l)}$  denotes the two-way signal propagation time from the  $n$ th antenna location to the  $(k, l)$ th pixel. Vector  $\mathbf{r}$  can be seen as the output of a weighted indicator function, which takes the value  $\sigma_p$  if the  $p$ -th point target exists at the  $(k, l)$ th pixel; otherwise, it is zero.

Eqn. (2) considers the contribution of only one sensor location. Stacking the measurement vectors corresponding to all  $N$  antennas to form a tall vector  $\mathbf{y}$ ,

$$\mathbf{y} = [\mathbf{y}_0^T \quad \mathbf{y}_1^T \quad \dots \quad \mathbf{y}_{N-1}^T]^T \quad (4)$$

we obtain the linear system of equations

$$\mathbf{y} = \Psi \mathbf{r} \quad (5)$$

where

$$\Psi = [\Psi_0^T \quad \Psi_1^T \quad \dots \quad \Psi_{N-1}^T]^T \quad (6)$$

## 3. SPARSIFYING DICTIONARY FOR IMAGING OF BUILDING STRUCTURES

Conventional CS-based TWRI operates under the point target model described in Section 2 and applies the sparsity condition directly to the scene  $\mathbf{r}$ , arguing that the number of point targets  $P$  is usually much smaller compared to the scene dimensions, i.e.  $P \ll N_x N_z$ . However, as we will see in Section 5, the underlying assumptions may not be satisfied when extended targets, such as walls, are present in the scene. This renders the imaging of building layout using conventional compressive sensing very challenging. We address this problem by designing a sparsifying dictionary based on Radon Transform, which exploits prior information based on common building construction practices.

The Radon Transform of a 2D image  $r(k, l)$ ,  $k = 0, \dots, N_x - 1$ ,  $l = 0, \dots, N_z - 1$ , projects the image along a specified line, and is defined as [7]

$$g(\rho, \theta) = \sum_{l=0}^{N_z-1} \sum_{k=0}^{N_x-1} r(k, l) \delta(\rho - k \cos(\theta) - l \sin(\theta)) \quad (7)$$

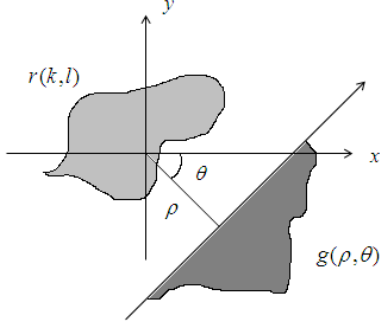


Fig. 2. Radon Transform

where  $\delta(\cdot)$  is the Dirac delta function, and  $\rho$  and  $\theta$  are the distance of the line from the origin and the angle from the horizontal, respectively (See Fig. 2).

In TWRI, the radar interrogates the scene usually along a line parallel to the front wall. Since it is common practice to build walls either parallel or perpendicular to each other, all walls present in the scene are assumed to be parallel or perpendicular to the sensors. Further, as only walls parallel to the sensor array appear in the image, we focus primarily on the detection of interior walls parallel to the front wall. This corresponds to the RT for  $\theta_0 = 90^\circ$ . Under these assumptions, the expression (7) reduces to,

$$g(\rho, \theta_0) = \sum_{k=0}^{N_x-1} r(k, \rho) \quad (8)$$

Each value of  $\rho$  represents a possible horizontal wall location in the image domain. The number of horizontal walls is typically much smaller compared to the down-range extent of the building,  $g(\rho, \theta_0)$  can be considered as sparse. Note that although other indoor targets, such as furniture and humans, may be present in the scene, their projections onto the horizontal lines are expected to be negligible compared to those of the wall.

In order to obtain a linear matrix-vector relationship between the scene and the horizontal projections, let us define a dictionary matrix  $\mathbf{R}$  composed of possible wall locations. Specifically, each of the columns of the dictionary  $\mathbf{R}$  represents an image containing a single wall located either in the left half or the right half of the image at a specific down-range (see Fig. 3)<sup>1</sup>. Therefore, the dimension of  $\mathbf{R}$  is  $N_x N_z \times 2D$ , where  $D$  denotes the number of possible wall down-range locations. Defining  $\hat{g}^{(1)}(\rho_i) = \frac{2}{N_x} \sum_{k=0}^{N_x/2-1} r(k, \rho_i)$  and  $\hat{g}^{(2)}(\rho_i) = \frac{2}{N_x} \sum_{k=N_x/2}^{N_x-1} r(k, \rho_i)$  for the left half and the right half of the image, respectively, and using  $\hat{\mathbf{g}} =$

<sup>1</sup>Note that we are implicitly assuming that the walls in the scene are linear combinations of half walls. In future work, we will study the relationship between the strength of the non-zero components of  $\hat{g}(\rho)$  and the wall extent to relax this condition.

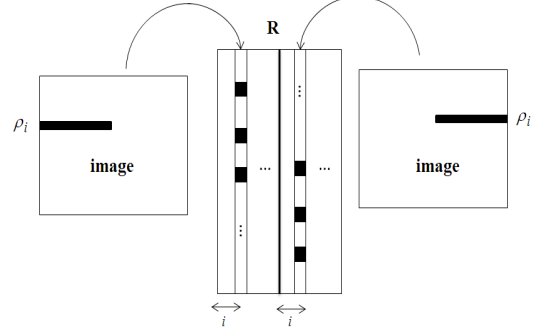


Fig. 3. Sparsifying dictionary generation.

$[\hat{g}^{(1)}(\rho_1) \dots \hat{g}^{(1)}(\rho_D) \hat{g}^{(2)}(\rho_1) \dots \hat{g}^{(2)}(\rho_D)]^T$ , we obtain

$$\mathbf{r} = \mathbf{R}\hat{\mathbf{g}} \quad (9)$$

In practice, the extension of the half wall patterns defined in  $\mathbf{R}$  are forced to be equal to half the extension of the front wall.

#### 4. IMAGING OF WALLS USING REDUCED DATA VOLUME

Substituting eqn. (9) in eqn. (5), we obtain the linear relationship between the projections of the horizontal walls and the through-the-wall radar measurements,

$$\mathbf{y} = \Psi \mathbf{R}\hat{\mathbf{g}} \quad (10)$$

Note that the above expression is based on the full data volume, i.e. measurements made at all  $N$  array locations using the  $M$  frequencies. Towards the objective of fast data acquisition, consider  $\check{\mathbf{y}}$ , which is a vector of length  $Q_1 Q_2 \ll MN$  consisting of elements chosen from  $\mathbf{y}$  as follows,

$$\check{\mathbf{y}} = \Phi \mathbf{y} \quad (11)$$

where  $\Phi$  is a  $Q_1 Q_2 \times MN$  matrix of the form,

$$\Phi = \text{kron}(\vartheta, \mathbf{I}_{Q_1}) \cdot \text{diag}\{\varphi^{(0)}, \dots, \varphi^{(N-1)}\} \quad (12)$$

In eqn. (12), ‘kron’ denotes the Kronecker product,  $\mathbf{I}_{Q_1}$  is a  $Q_1 \times Q_1$  identity matrix,  $\vartheta$  is a  $Q_2 \times N$  measurement matrix constructed by randomly selecting  $Q_2$  rows of an  $N \times N$  identity matrix, and  $\varphi^{(n)}$ ,  $n = 0, 1, \dots, N-1$ , is a  $Q_1 \times M$  measurement matrix constructed by randomly selecting  $Q_1$  rows of an  $M \times M$  identity matrix. We note that  $\vartheta$  determines the reduced antenna locations, whereas  $\varphi^{(n)}$  determines the reduced set of frequencies corresponding to the  $n$ th antenna location.

Given  $\check{\mathbf{y}}$ , we can recover  $\hat{\mathbf{g}}$  by solving the following equation,

$$\check{\mathbf{g}} = \arg \min_{\mathbf{x}} \|\mathbf{x}\|_{l_1} \quad \text{subject to} \quad \check{\mathbf{y}} \approx \Phi \Psi \mathbf{R}\mathbf{x} \quad (13)$$

Several methods are available in the literature to solve the optimization problem in (13). In this paper, we choose Orthogonal Matching Pursuit (OMP) to solve (13), which is known to provide a fast and easy to implement solution. Finally, the scene can be reconstructed using the estimated sparse vector  $\hat{\mathbf{g}}$  through a simple multiplication  $\hat{\mathbf{r}} = \mathbf{R}\hat{\mathbf{g}}$ .

## 5. SIMULATION AND EXPERIMENTAL RESULTS

### 5.1. Simulation Results

In this section, we evaluate the performance of the proposed scheme using synthesized data. A stepped-frequency signal consisting of 335 frequencies covering 1-2 GHz was used. A 71-element monostatic array with an inter-element spacing of 2.2cm was employed. The array is located parallel to a 1.83m-wide front wall centered at 0m in cross-range. The scene behind the front wall contains two half walls and a single point target. The first wall extends from 0 to 0.95m in cross-range at a downrange of 4.4m, while the second wall is located at 5.61m downrange, extending from -0.95m to 0m in cross-range. The location of the point target is (-0.47, 3.82)m. Fig. 4 depicts the geometry of the simulated scene. The region to be imaged is chosen to be 4.9m (cross-range)  $\times$  4.3m (down-range), centered at (0, 2.15)m, and is divided into  $73 \times 73$  pixels.

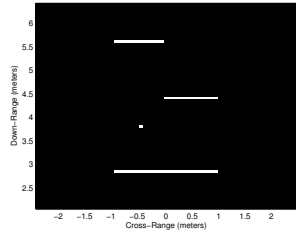


Fig. 4. Geometry of the simulated scene

Fig. 5(a) shows the backprojected image using all  $MN$  observations. The three walls and the point target are clearly visible. However, when only 1% of the full data volume (10% randomly selected frequencies and 10% randomly chosen sensor locations) is considered, backprojection produces the image shown in Fig. 5(b). Clearly, data reduction translates into the appearance of several false targets, thereby impeding the detection of the building layout.

The proposed method was applied to the reduced set of measurements and the recovered sparse vector  $\hat{\mathbf{g}}$  is depicted in Fig. 6. Four peaks corresponding to the true wall locations can be clearly seen. Fig. 7(a) shows the corresponding reconstructed scene, which depicts the front wall and the two interior walls. For comparison, the image reconstructed with the conventional CS-based imaging, with an assumed sparsity of 4, using the reduced data volume is provided in Fig. 7(b). Since the walls are extended targets and appear dense

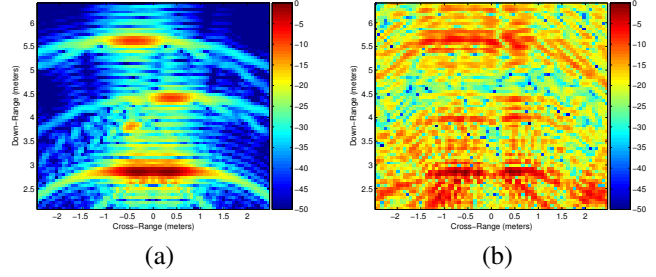


Fig. 5. Backprojected image: (a) full dataset, (b) 1% of the data volume.

under the point target model, the conventional CS approach populates four pixels located on the front wall and is, thus, not suited for building layout reconstruction.

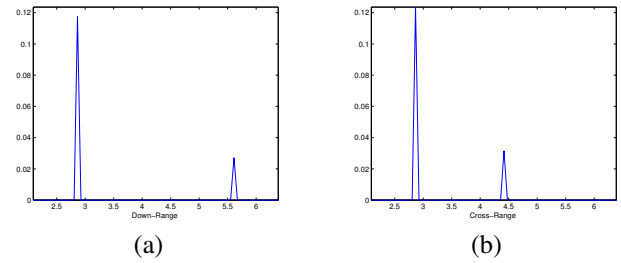


Fig. 6. Recovered sparse vector  $\hat{\mathbf{g}}$ : (a) Left half walls, (b) Right half walls.

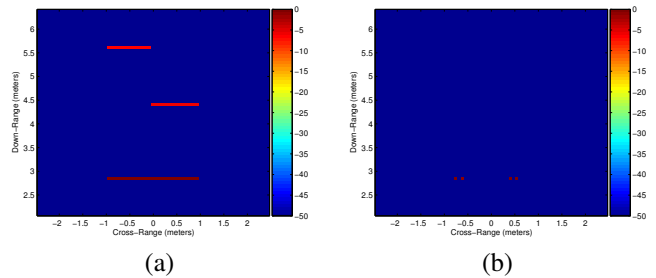
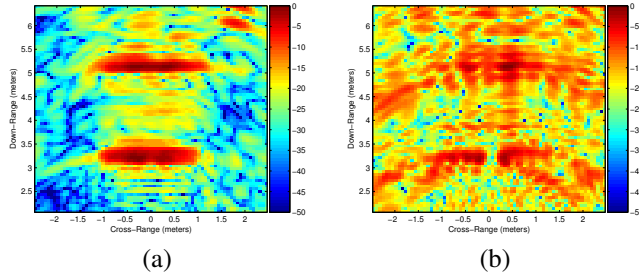


Fig. 7. Recovered images using 1% of the data samples: (a) Proposed method, (b) Conventional CS

### 5.2. Experimental Results

A through-the-wall SAR system was set up in the Radar Imaging Lab, Villanova University. The system and signal parameters are the same as those for the simulated data. The scene consists of two parallel plywood walls, each 2.25cm thick, 1.83m wide, and 2.43m high. Both walls are centered at 0m in cross-range. The first and the second walls are located at respective distances of 3.25m and 5.1m from

the antenna baseline. Fig. 8(a) shows the backprojected image using the full dataset, wherein the walls can be clearly seen. For compressive sensing, we consider 25% randomly selected frequencies and 25% randomly chosen sensor locations, which represent 6.3% of the full data volume. Similar to the simulated case, the backprojected image corresponding to the reduced data, shown in Fig. 8(b), suffers from several false alarms.



**Fig. 8.** Backprojected image: (a) full dataset, (b) 6.3% of the data volume.

The sparse vector  $\hat{\mathbf{g}}$  estimated from the reduced data using the proposed method is depicted in Fig. 9, where four peaks associated with the true walls (two half walls for each wall present in the scene) can be identified. The corresponding image is shown in Fig. 10(a), which shows that the two walls have been successfully reconstructed even though the number of measurements has been significantly reduced. When conventional CS-based imaging is used to reconstruct the image with an assumed sparsity of four, it fails to recover the two walls, as shown in Fig. 10(b).

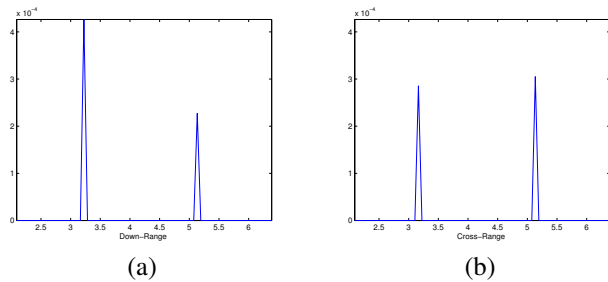


**Fig. 9.** Recovered sparse vector  $\hat{\mathbf{g}}$ : (a) Left half walls, (b) Right half walls.

## 6. CONCLUSION

A sparsity-based approach for imaging of interior building structure has been presented. The proposed technique takes advantage of the prior information about building construction practices to design a sparsifying dictionary based on the expected wall alignment relative to the radar’s scan direc-

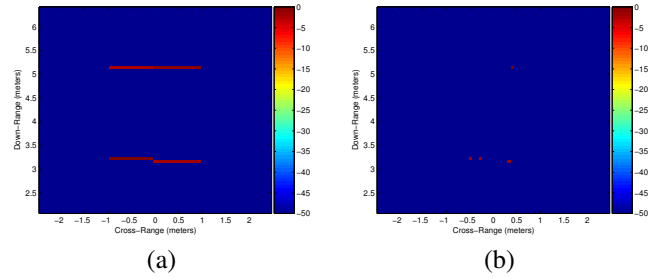


**Fig. 10.** Recovered images using 6.3% of the data samples: (a) Proposed method, (b) Conventional CS

tion. The proposed method provides reliable determination of building layouts while achieving substantial reduction in data volume. Results based on laboratory experiments were presented, which depicted the superior performance of the proposed method compared to backprojection and conventional point-target based compressive sensing.

## 7. REFERENCES

- [1] M. Amin and K. Sarabandi (Eds.), “Special issue on Remote Sensing of Building Interior,” *IEEE Trans. Geosci. Remote Sens.*, vol. 47, no. 5, pp. 1270–1420, 2009.
- [2] D.L. Donoho, “Compressed sensing,” *IEEE Trans. Inf. Theory*, vol. 52, no. 4, pp. 1289–1306, 2006.
- [3] F. Ahmad (Ed.), *Compressive Sensing*, Proc. of SPIE, vol. 8365, SPIE, Bellingham, WA, 2012.
- [4] Y.S. Yoon and M. Amin, “Compressed Sensing Technique for High-Resolution Radar Imaging,” *Proc. SPIE*, vol. 6968, pp. 69681A–1–69681A–10, 2008.
- [5] C. Debes, M. Amin, and A.M. Zoubir, “Target Detection in Single- and Multiple-View Through-The-Wall Radar Imaging,” *IEEE Trans. Geosci. Remote Sens.*, vol. 47, no. 5, pp. 1349–1361, May, 2009.
- [6] F. Ahmad and M. Amin, “Matched-Illumination Waveform Design for a Multistatic Through-the-Wall Radar System,” *IEEE J. Sel. Topics Signal Process.*, vol. 4, no. 1, pp. 177–186, 2010.
- [7] P. Toft, “The Radon Transform - Theory and Implementation,” *Ph.D. thesis, Technical U. of Denmark*, 1996.
- [8] A.C. Gurbuz, J.H. McClellan, and W.R. Scott, “Compressive Sensing of underground structures using GPR,” *Digital Signal Process.*, vol. 22, no. 1, pp. 66–73, 2012.
- [9] M. Aftanas and M. Drutarovsky, “Imaging of the Building Contours with Through the Wall UWB Radar System,” *Radioeng. J.*, vol. 18, no. 3, pp. 258–264, 2009.